J Geophys (1981) 50: 51–67

Journal of Geophysics

Characteristics of Westward Travelling Surges During Magnetospheric Substorms

W.G. Tighe and G. Rostoker
Institute of Earth and Planetary Physics and Department of Physics, University of Alberta, Edmonton, Alberta, Canada T6G 2J1

Abstract. Data from arrays of magnetometers along lines of constant magnetic latitude and longitude supplemented by all-sky camera and riometer data are used to infer the characteristics of the temporal development and the typical scale size of westward travelling surges which occur during magnetospheric substorms. It is found that the motion of the head of the surge can be quite irregular, and that in extreme cases the surge form may grow and decay in a confined longitudinal sector without suffering any significant westward displacement. The positive *D*-component perturbation, known to be the characteristic signature of a surge, is generally confined within a longitude range of ~6–10° at ~70° N and is thought to be generated by a filamentary southward ionospheric current flowing at the head of the surge. A comprehensive model three-dimensional current system involving this equatorward current and northwestward current flow in the region to the east of the head of the surge is presented through a detailed comparison of model and observed latitude and longitude profiles of the magnetic disturbance. It is found that best agreement is obtained when the entire electrojet system flows from southeast to northwest relative to the lines of constant magnetic latitude.

Key words: Auroral zone magnetic fields – Westward travelling surge – Three-dimensional current system – Auroral electrojet – Substorm

Introduction

The magnetospheric substorm is a large scale episode of enhanced energy dissipation in the ionosphere reflected by marked increases in auroral luminosity, acceleration of electron and ions and significant joule heating due to increased current flow in the auroral zone electrojets. The concept of the substorm was developed by Akasofu (1964) for the auroral signatures, and has subsequently been extended to encompass associated variations in particles, current and electromagnetic noise in various portions of the frequency spectrum (Akasofu 1968). The substorm has only just recently been given an operational definition (Rostoker et al. 1980) in which multiple surges and associated current intensifications are permitted to occur inside the time frame of a single substorm. In this paper we will be addressing the problem of the development of the auroral and electric current features during individual intensifications within the body of a substorm.

The westward travelling surge is a well recognized signature of the magnetospheric substorm which is thought to represent the western edge of the substorm disturbed region. The surge moves erratically in a northwest direction during the course of a substorm (Wiens and Rostoker 1975) although individual surge features may expand smoothly westward and surge forms will sometime develop to the east of the head of the westward electrojet (Pytte et al. 1976). There have been several detailed studies of the auroral and magnetic field signatures of surges (Akasofu et al. 1966; Meng 1965; Kisabeth and Rostoker 1973; Chen and Rostoker 1974; Rostoker and Hughes 1979; Baumjohann 1979) which have provided an important base of knowledge regarding the phenomenonology of this substorm feature. Kisabeth and Rostoker (1973) have shown that the positive perturbation of the *D* (east-west) component of the magnetic field is a primary feature of the disturbance region and Rostoker and Hughes (1979) have reached the conclusion that this feature is due to an equatorward ionospheric current flowing at the head of the surge. However, lack of adequate ground based magnetometer coverage has, till now, prevented a detailed study of the westward propagation of the surge from being carried out. Over the past 5 years the University of Alberta has intermittently operated an east-west line of between three and four magnetometers along a line of constant geomagnetic latitude (~67.3° N) over an east-west extent of ~12° of longitude. For some of this time an all-sky camera was operated at Forth Smith (SMIT) so that concurrent information on auroral luminosity was available for some events. For other events, riometer data were available which allowed the region of energetic electron precipitation to be studied. In this paper we use the above-mentioned data base to study the development and propagation of westward travellling surges, and we further present model three-dimensional current systems which we believe to be capable of producing the surge magnetic field perturbations in terms of both spatial motion and temporal intensity variations.

Presentation of the Data

In our study we have explored the development of twelve substorm events in which surge forms were detected in the Alberta sector. Tighe (1979) has analysed three of these events and in our paper we shall present detailed analyses of two of these events. For the first event on Day 214, 1974 the University of Alberta magnetometer array involved the stations of Uranium City, Fort Smith and Hay River spaced at intervals of ~5° along a line of constant geomagnetic latitude at ~67.3° N. Supplementary data available from standard observatories operated by Dept. of Energy, Mines and Resources (Earth Physics Branch), were used in the study, along with all-sky camera data

0340-062X/81/0050/0051/$03.40

Table 1. Locations of stations used in this study

Station name	Code name	Geographic coordinates		Geomagnetic coordinates	
		Lat.	Long.	Lat.	Long.
Uranium City	URAN	59.6	251.5	67.4	304.3
Forth Smith	SMIT	60.0	248.0	67.3	299.7
Hay River	HAYR	60.8	244.2	67.3	294.1
Fort Providence	PROV	61.3	242.4	67.5	292.0
Fort Chipewyan	CHIP	58.8	248.9	66.3	302.1
Fort McMurray	MCMU	56.8	248.8	64.2	303.2
Leduc	LEDU	53.3	246.5	60.6	302.9
Cambridge Bay	CAMB	69.1	255.0	76.7	294.0
Yellowknife	YKNF	62.5	245.5	69.1	292.6
Meanook	MEAN	54.6	246.7	61.8	301.0
Fort Churchill	CHUR	58.8	265.8	68.8	322.5
Whiteshell		49.8	264.8	59.9	325.9
Great Whale River		55.3	282.2	66.8	347.2
Victoria		48.5	236.8	54.3	292.7
College		64.9	212.2	64.6	256.5
Sitka		57.1	224.7	60.0	275.4
Newport		48.3	242.9	55.1	300.0
Boulder		40.1	254.8	49.0	316.5
Honolulu		21.3	202.0	21.1	266.5

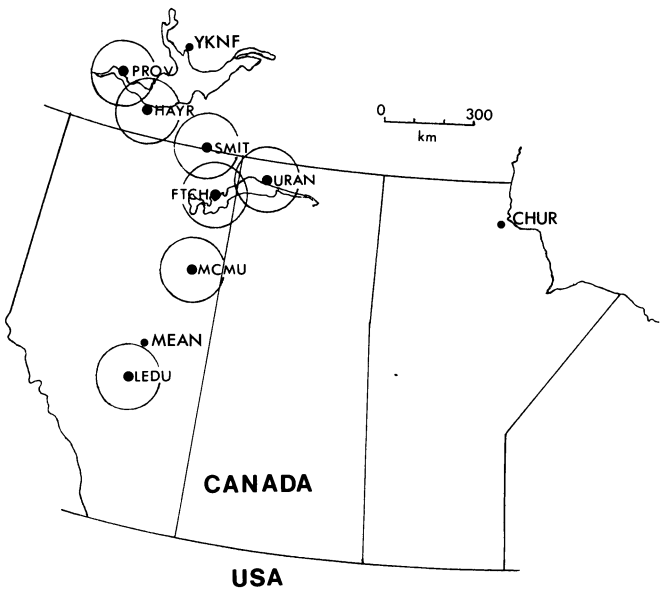

Fig. 1. Station locations of the University of Alberta magnetometers and riometers and other selected stations in the Alberta sector. The *circles* indicate the field of wiew of the riometers. The station code names and geomagnetic coordinates are given in Table 1

from Forth Smith. For the second event on Day 307, 1976 the IMS array was operative, with data being available from an east-west line along ~67.3° N stretching over ~12° from Uranium City to Forth Providence and along a meridian ~300° E from Leduc in the south to Cambridge Bay in the north. Riometer data from Fort Providence, Hay River, Fort Smith and Fort McMurray were available as well for this event. Station coordinates and code names used in this study are shown in Table 1 and the station locations are shown in Fig. 1.

The data are presented in the following formats: (i) The magnetometer data are shown in their classical magnetogram format, stacked in each figure so as to facilitate easy comparison among the traces and to portray the evolution in time of the event. A coordinate transformation of the data results in the traces being representative of the north-south (H'), east-west (D') and vertical components Z in the centered dipole coordinate system. The magnetometer data are also portrayed in the profile format for a given instant in time. *Latitude profiles* involve perturbations from stations which lie along a line of constant geomagnetic longitude, while *longitude profiles* involve perturbations from stations which lie along lines of constant geomagnetic latitude. Both these profiles permit one to evaluate the spatial character of the substorm current flow at a given instant of time. The baseline for substorm events is chosen in the minute or so prior to onset, and is changed for each subsequent intensification to the minute prior to the intensification – such profiles have been termed differential profiles (Kisabeth 1972). (ii) The riometer data are shown as stacked time series, which indicate the level of the signal in terms of dB. (iii) The all-sky camera data are shown as linear mappings of the auroral images recorded at 30 s intervals using alternate 8 and 16 s exposure times.

The Substorm Surge Events

(i) Day 214 (2 August, 1974)

The event in question appears to have its onset at ~0626 (all times in this paper are given in universal time) after a sustained period of quietness. The stacked magnetograms for the H', D', and Z components are shown in Fig. 2a–c respectively. There is some indication of a slow buildup of electrojet strength starting around 0620, however the distinctive arc brightening identifying the substorm onset (Akasofu 1964) does not occur until 0626. The auroral mappings and matching longitude profiles of the magnetic data are shown in Fig. 3a, b. The arrows a, b, c, ... in Fig. 2 pertain to the auroral mappings A, B, C, . in Fig. 3.

The substorm onset features a negative H' perturbation at the eastern stations of URAN and CHUR. CHUR shows a marked $+D'$ perturbation indicating it is near the head of the surge, while the Alberta array registers a small $-D'$ disturbance indicating it is not in the region of the surge. It is interesting to note the appearance of the surge form ~200 km to the east of URAN does not produce the familiar $+D'$ signature at that station suggesting that the $+D'$ surge signature may be quite localized spatially. In fact all three stations in the Alberta array show rather small magnetic perturbations in this phase of the substorm.

The appearance of the surge at the eastern edge of the Alberta array at ~0628 is accompanied by a sharp $+D'$ pertubation at URAN. This signature is slightly delayed at SMIT (implying some propagation delay) and is completely absent at HAYR (indicating that the effects of the surge are not felt that far west). The all-sky data in Fig. 3 indicate that the main surge form has moved to about 100 km east of URAN and that the arc structure has developed a perturbed character between URAN and SMIT. The buildup of $-H'$ at URAN as indicated by the longitude profile in Fig. 3a indicates that the western edge of the westward electrojet has moved closer to URAN in the two minutes since onset. By ~0630 the western edge of the surge has moved to between URAN and SMIT Here we really can see the localized nature of the $+D$ disturbance for profile C. Initially URAN fails to respond, and then drops negatively while SMIT registers the $+D$ spike and HAYR still fails to respond. The longitude profile at 0629:57 is typical for that associated with a Birkeland current loop involving down-

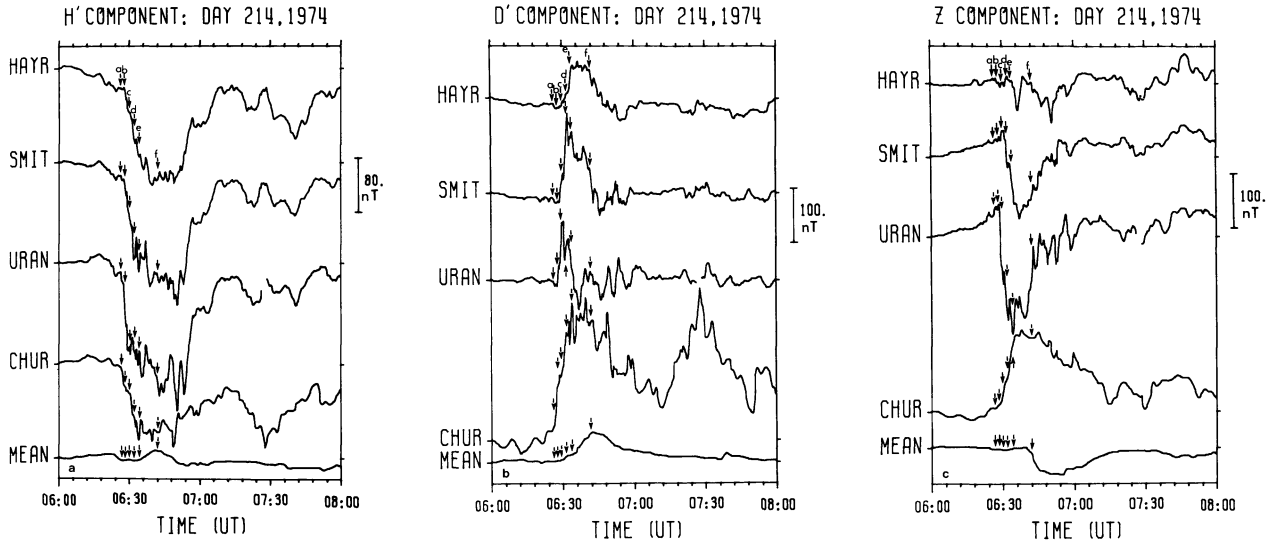

Fig. 2a–c. Stackplots of magnetograms from central and western Canadian stations covering the substorm event of day 214, 1974. The *arrows* labelled *a, b,...* indicate specific instants during the substorm which are referred to in the text and in Fig. 3. **a** for the H'-component, **b** for the D'-component, **c** for the Z-component

ward field-aligned current at the north linked to upward field-aligned current to the south by equatorward ionospheric current (see Fig. 3 of Kawasaki and Rostoker (1979a)). The negative H' in the profile indicates further westward expansion (and possibly intensification) of the westward electrojet. By ~0632 the surge is over SMITH with its western edge reaching to within ~50 km from HAYR. At this time the D' component goes sharply positive at HAYR, SMIT and URAN showing all three stations to be under the influence of the surge. By ~0634 the active arcs have moved to the west of the Alberta array leaving the stations under the influence of a westward electrojet whose intensity does not seem to vary much with longitude (as seen from profiles D and E in Fig. 3).

This event features a surge which developed to the east of the Alberta array and which moved between ~0626–0631 across the array with a relatively smooth westward motion. Between ~0631–0633 the surge form became stationary, but at 0633 it jumped suddenly westward. This motion is inferred by studying the position of the leading edge of the surge as a function of time as shown in Fig. 4. Since we associate the $+D'$ magnetic disturbance with the surge form, it was useful to study the motion of a well defined feature in the D'-component longitude profile, this being the position of the polarity reversal in D' which can be seen in frame B of Fig. 3. The position of the polarity reversal was studied at 10 second intervals and is shown in Fig. 4 for comparison with the position of the head of the surge as inferred from the auroral luminosity. Clearly, over the period during which the surge was over the Alberta array, the slope of the two curves is approximately the same with regression analysis yielding a velocity of 1.9 ± 0.2 km/s for the auroral feature and 2.3 ± 0.2 km/s for the D'-component crossover. Given the errors of up to 5% in the scaling factors used in transposing the all-sky camera photos to linear mappings, this agreement can be considered to be rather good.

In summary, we have shown an example where the surge moved from the eastern field of view over the Alberta array. The motion is smooth for ~5 minutes between 0626 and 0631, but was absent for two minutes between 0631 and 0633 after which time rapid westward motion was again initiated. Inspection of the longitude profiles indicate a regime of negative D' to the west of the surge and a region of positive D' under the surge. There is some indication of negative D' behind the surge (see SMIT and URAN in Fig. 2b) but this is not well pronounced for this event. The Z-component is positive to the west of the surge and negative to the east of the surge. The H' component is negative under the surge and to the east of it, indicating the effect of the substorm westward electrojet. The Z and D' profiles are what one would expect from a three-dimensional current system involving anti-parallel Birkeland current sheets connected by ionospheric equatorward current flow.

(ii) Day 307 (2 November, 1976)

The substorm analysed in this section features the development and decay of several surge features which appear in different positions with respect to the Alberta array. Magnetograms from the east-west line are shown in Fig. 5 with records from the north-south line within the Alberta array being shown in Fig. 6 and riometer data from the Alberta array being shown in Fig. 7.

The substorm onset occurred at ~0625 as evidenced from the negative H' component perturbations visible across the Alberta sector. A latitude profile taken shortly after the substorm onset is shown as panel A of Fig. 8. The substorm westward electrojet is seen to lie in the latitude range ~65°–69°. The lack of a positive D'-component perturbation indicates that the surge has not penetrated the Alberta sector at this time. This would suggest that the magnetic perturbations stem from enhanced current flow in the discrete auroral arc region immediately to the west of the substorm disturbed region (Kawasaki and Rostoker 1979b). The longitude profile for the same instant of time (panel A of Fig. 9) is consistent with this view in that it shows a negative H'-component perturbation which changes little across the east-west extent of the Alberta array. In addition, the east-west gradient in the Z-component and the steady negative D'-component perturbation indicate a westward jet which is tilted $15° \pm 5°$ to the north-west over the interval 0625–0640 (period A on the magnetograms).

At ~0640 the structure of the current flow in the Alberta sector is altered significantly by the growth of a surge structure. Initially the structure is highly localized near SMIT as one can

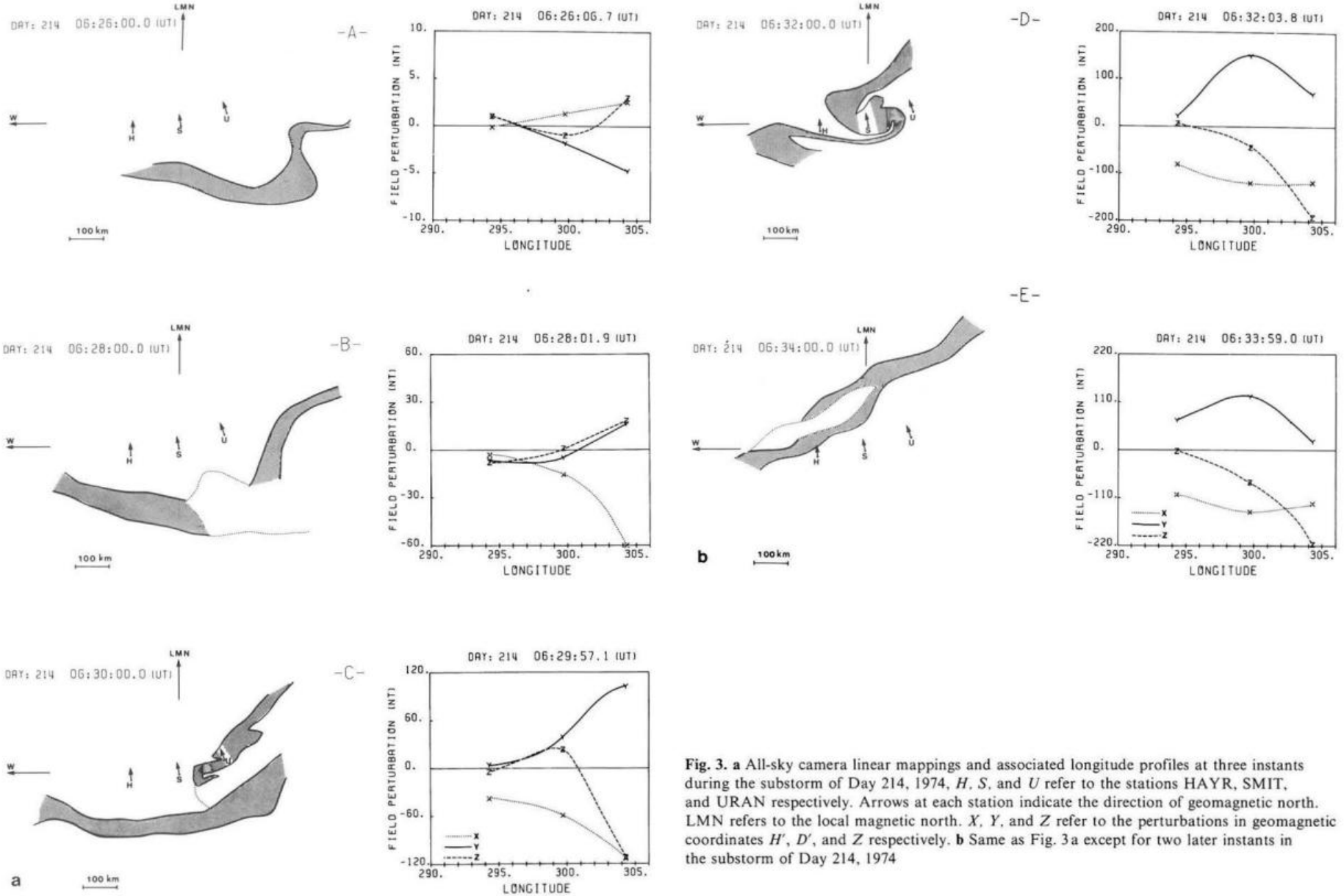

Fig. 3. a All-sky camera linear mappings and associated longitude profiles at three instants during the substorm of Day 214, 1974, *H*, *S*, and *U* refer to the stations HAYR, SMIT, and URAN respectively. Arrows at each station indicate the direction of geomagnetic north. LMN refers to the local magnetic north. *X*, *Y*, and *Z* refer to the perturbations in geomagnetic coordinates *H'*, *D'*, and *Z* respectively. **b** Same as Fig. 3a except for two later instants in the substorm of Day 214, 1974

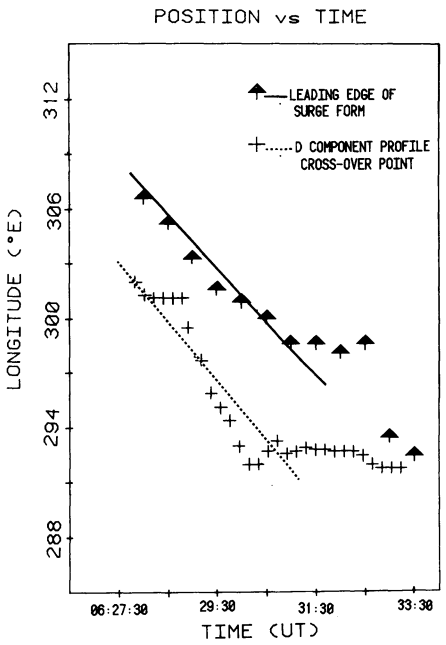

Fig. 4. Graph of the average position of the leading edge of the surge and the position of the polarity reversal in the D'-component (from negative in the west to positive in the east) as a function of universal time. Note the abrupt cessation of westward motion at ~0630

see comparing the D'-component perturbations to the east, west and south of SMIT to that at SMIT itself. In addition there is a significant precipitation event at SMIT which is not present either at PROV or HAYR to the west (see Fig. 7). The latitude and lingitude profiles at two instants during the development of the surge are shown in panels B1 and B2 of Figs. 8 and 9. The tendency for the peak disturbance to remain localized at SMIT indicates that this surge form is not moving westward significantly. In fact, the perturbation pattern at URAN suggests that the surge did not move into the Alberta sector from the east. We conclude that this surge form has developed in a localized azimuthal sector centered near SMIT. While the disturbance has the magnetic signature of the westward travelling surge, this surge is not travelling but decays away while remaining relatively stationary.

From 0645–0650 (period C on the magnetograms) another surge form develops. Panel C of Figs. 8 and 9 show the latitude and longitude profiles at one instant during the development of the surge. It can be seen that the peak D'-component disturbance is now near HAYR, about 5° to the west of SMIT. Minute by minute profiles (not shown here) indicate, as in the case of period C, that the surge grows and decays while showing no discernable westward motion. Based on the data from the east-west line and the enhanced D'-component perturbations at YKNF (relative to the earlier periods A and B) we would say that this surge formed to the north and west of the previous one (event B).

The major intensification in this substorm takes place near 0656, with the D'-component data (Panel D1 of Fig. 10) showing the surge developing in the vicinity of SMIT. The latitude profiles (panels D1 and D2 of Fig. 11) indicate that the surge expands rapidly poleward in conjunction with the development of a strong westward electrojet at the poleward edge of the array. The longitude profiles in Figs. 10 and 12 document the development of the surge and suggest clear westward propagation. While the peak of the surge form is near SMIT at ~0656 (D1), it lies between HAYR and PROV by ~0659 (D2) and well to the west of PROV by ~0703 (D3). Based on the motion of the point at which the polarity of the D'-component reverses (e.g., the crossover point is ~300°–301° E in panel D3 of Fig. 10), the velocity of the surge is estimated to be ~1.2 km/s over the interval 0656–0703.

Following the passage of this major surge, the substorm continues to develop to the west of the Alberta array. Latitude and longitude profiles taken at 0718:35 (panel E in Figs. 11 and 12) show an intense electrojet peaking to the north of YKNF with a maximum H'-component perturbation of at least ~430 nT. The longitude profile shows an electrojet which features little longitudinal gradient in current intensity. The tilt in the Z-component profile taken together with the steady D-component perturbation can be used to estimate the angle which the electrojet makes with respect to lines of constant geomagnetic latitude. The estimated value of 20° ± 5° is close to the estimate

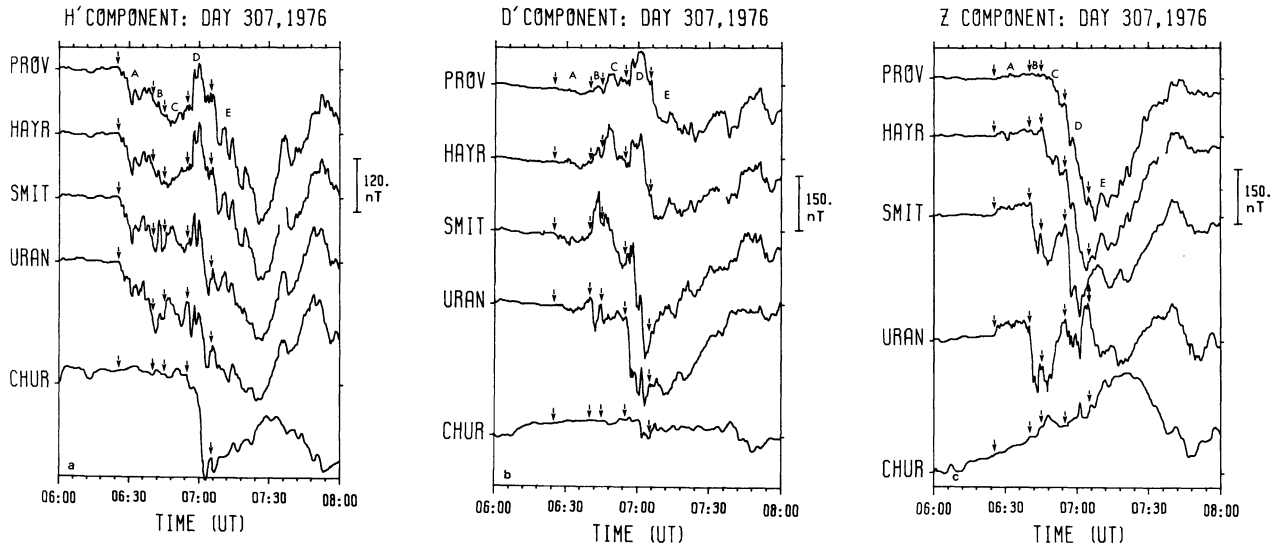

Fig. 5a–c. Stackplots of magnetograms along an east-west line stretching form PROV to CHUR for the substorm event of Day 307, 1976. The intervals *A*, *B*,... refer to specific intervals referred to in the text. **a** for the H'-component, **b** for the D'-component, **c** for the Z-component

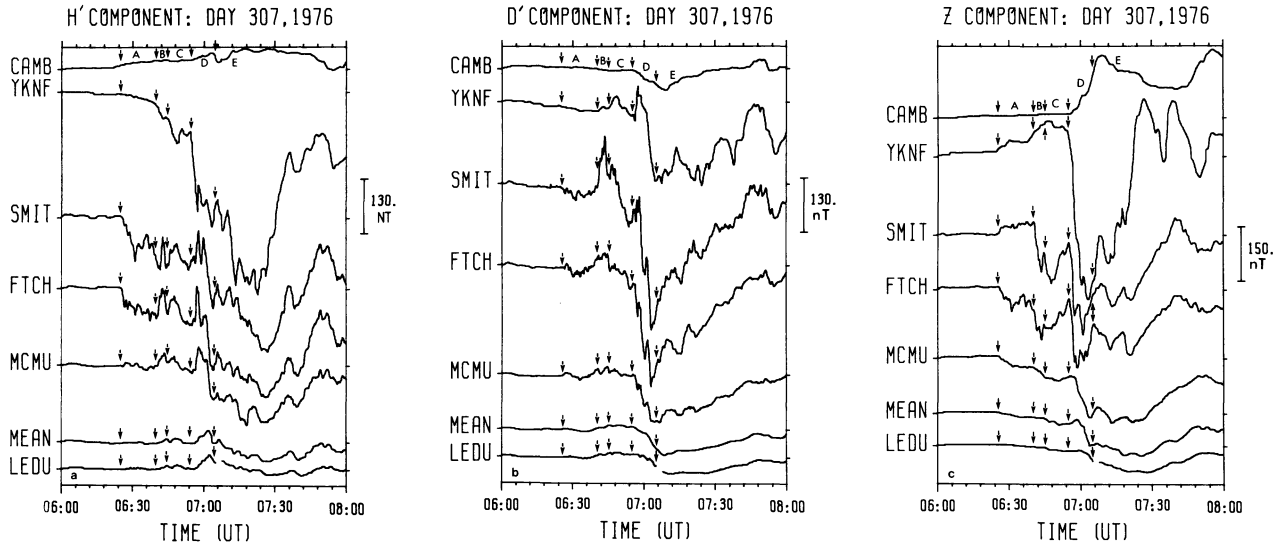

Fig. 6a–c. Stackplots of magnetograms along a north-south line through the Alberta sector for the substorm event of Day 307, 1976. **a** for the H'-component, **b** for the D'-component, **c** for the Z-component

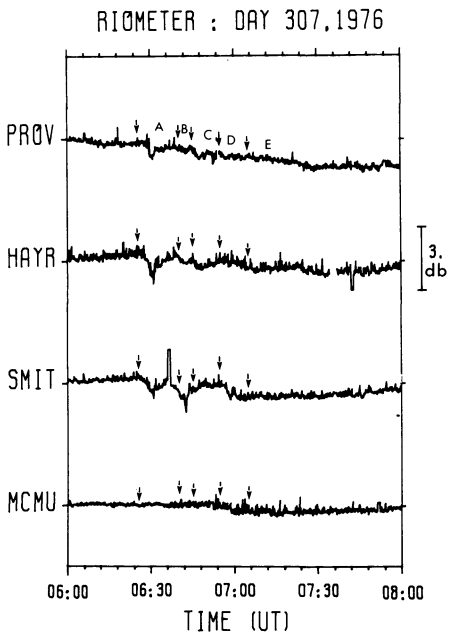

Fig. 7. Riometer data from four observatories in the Alberta sector recorded during the substorm event of Day 307, 1976. The intervals *A, B, ...* are referred to in Figs. 5 and 6 and in the text

of the angle which the electrojet made with lines of constant geomagnetic latitude ($\sim 15 \pm 5°$) at the very beginning of the substorm (period A). The passage of the substorm has not apparently influenced the gross configuration of the auroral oval over this time scale of ~ 1 h.

In summary, we have seen in this substorm an example of a surge which propagates westward and examples of surges which grow and decay while remaining relatively stationary. In addition we have seen a surge form develop to the east of a previous surge in the body of the same substorm, in agreement with earlier observations by Pytte et al. (1976).

Modelling of Substorm Surges

The data presented in this paper include the first longitude profiles of westward travelling surges. As such, it is worthwhile itemizing some of the characteristic features of the surge perturbation pattern with emphasis on changes which occur as a function of longitude. The reader is referred to Figs. 3, 9, 10 and 12 for examples of the longitude profiles on which our synthesis is based:

(a) The dominant feature is a regime of positive D' which earlier studies (Kisabeth and Rostoker 1973; Rostoker and Hughes 1979) have found to be in the near vicinity of the western edge (or head) of the surge. At the positive peak of D', the Z-component is normally negative, while the H'-component is either positive or negative depending on the position of the observing station with respect to the center of the surge.

(b) As one moves westward from the position of peak positive D', the D'-component falls off in magnitude eventually becoming slightly negative. As this happens Z becomes positive reaching a positive peak before falling off to zero. The H'-component tends to fall off toward zero as one moves westward from the position of peak positive D'.

(c) As one moves eastward from the position of peak positive D', the D'-component falls off toward zero eventually becoming negative. Normally the negative D' behind the surge is very large, often exceeding in value the magnitude of the peak positive D', although occasionally the magnitude of the negative D' perturbation can be small. The peak value of negative Z is normally obtained at the longitude where D' switches from being positive to being negative. The H'-component reaches its maximum negative values in the region east of the polarity transition in D'.

A schematic diagram of a typical surge longitude profile is shown in Fig. 13.

A cursory comparison of the schematic diagram shown in Fig. 13 with model current system magnetic perturbation patterns suggests that most of the disturbance on the western portion of the surge is due to a three-dimensional Birkeland current system with downward current at the poleward edge linked to upward current at the equatorward edge by equatorward flowing ionospheric current, as suggested by Rostoker and Hughes

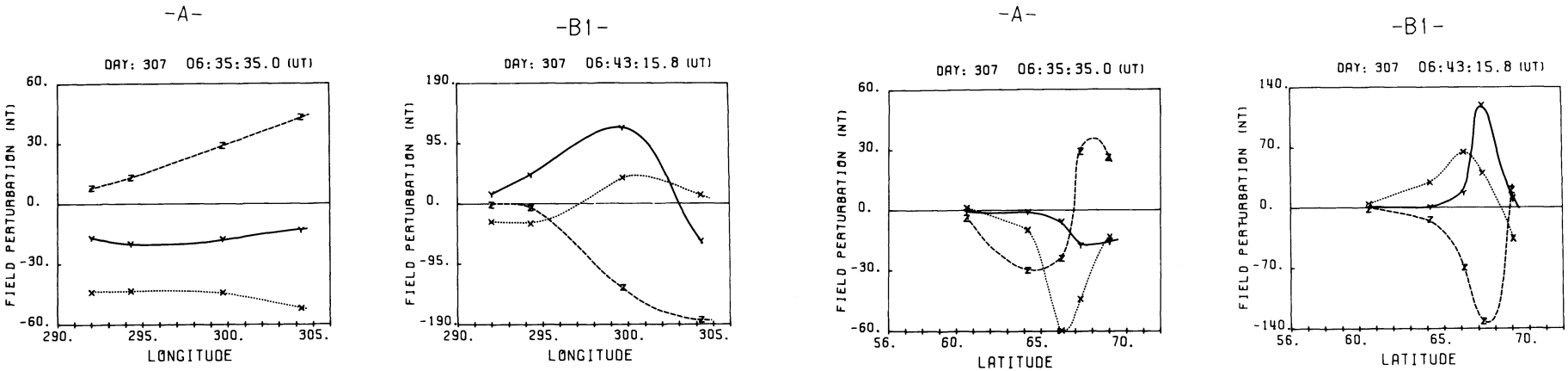

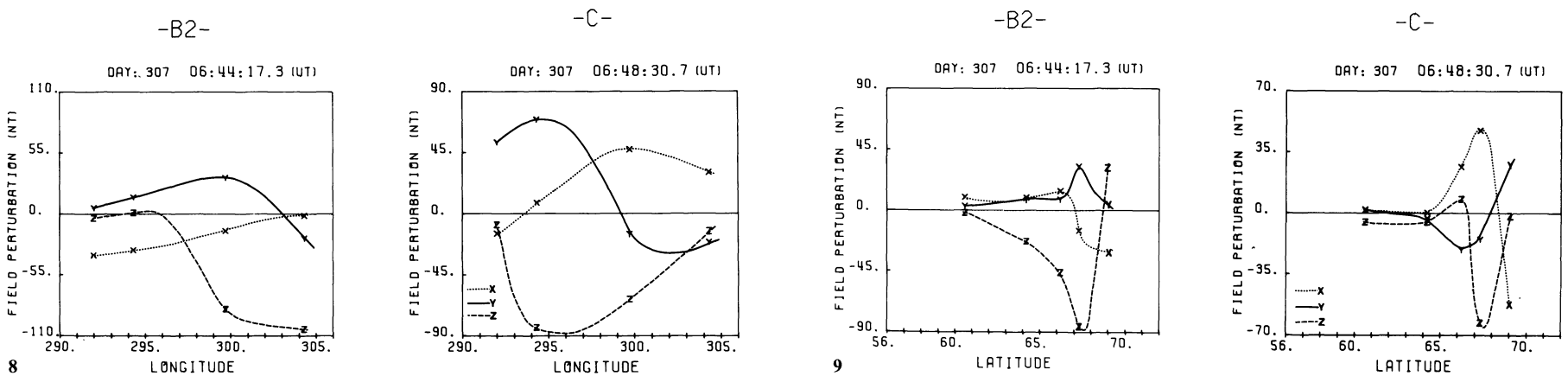

8 9

Fig. 8. Latitude profiles taken at instants during the intervals *A*, *B*, and *C* during the substorm of Day 307, 1976. The symbols *X*, *Y*, and *Z* refer to the perturbations in geomagnetic coordinates *H'*, *D'* and *Z* respectively

Fig. 9. Same as Fig. 8 except the corresponding longitude profiles are shown

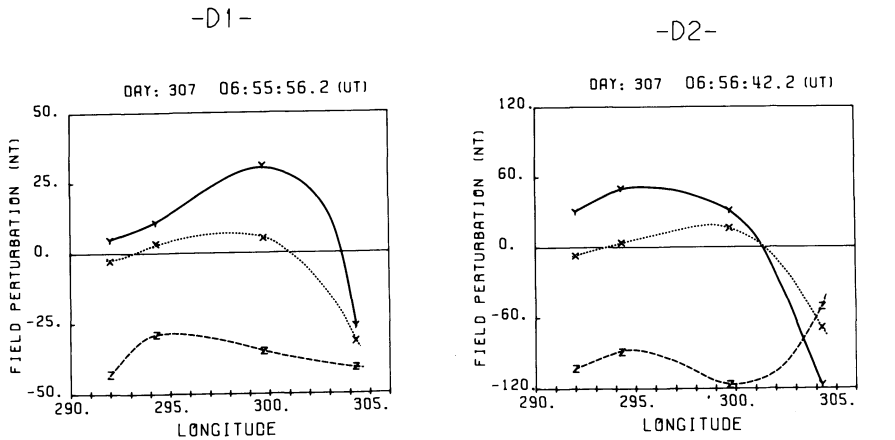

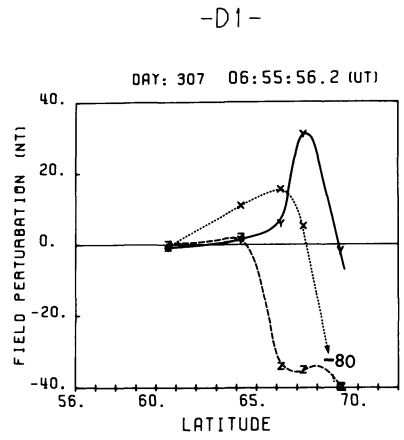

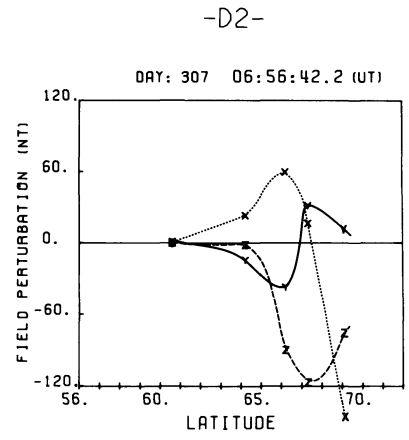

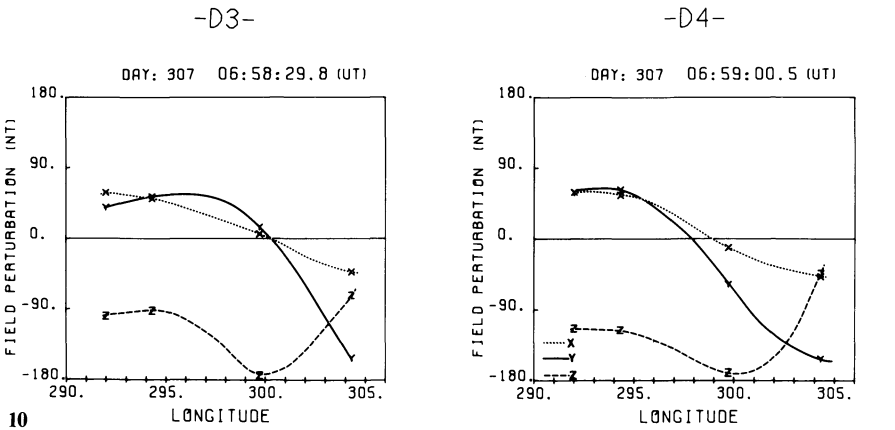

10

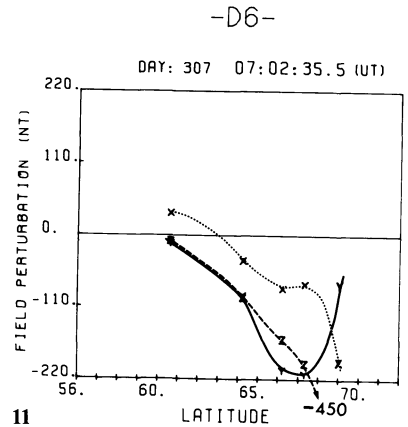

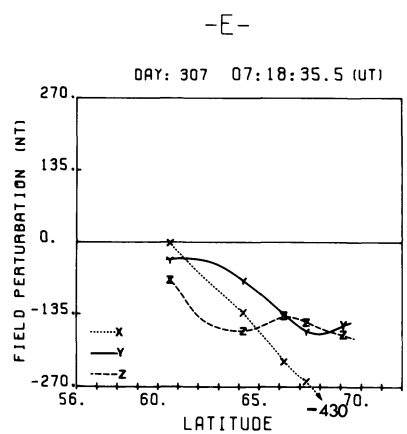

11

Fig. 10. Same as Fig. 9 except for instants during interval *D* of the substorm on Day 307, 1976

Fig. 11. Same as Fig. 8 except for instants during interval *D* of the substorm on Day 307, 1976

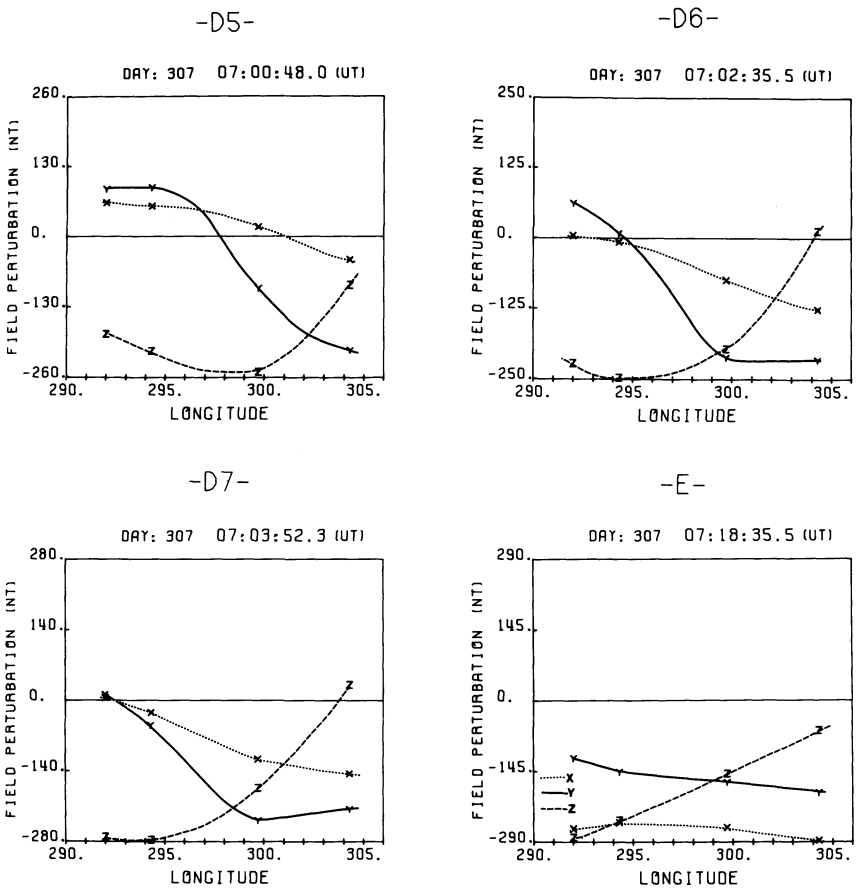

Fig. 12. Same as Fig. 9 except for instants during intervals *D* and *E* of the substorm on Day 307, 1976

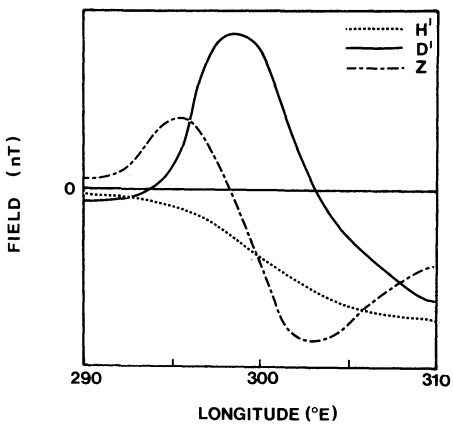

Fig. 13. Schematic diagram at a typical surge longitude profile in accordance with the observations reported in this paper

(1979). The perturbation pattern as a function of longitude for such a system is shown in Fig. 14. It is immediately apparent that the major differences between Figs. 13 and 14 are in the region to the east of the head of the surge. Those differences can, in the main, be explained by the presence of the westward electrojet for which the surge is the leading head. Two schematic profiles are shown in Fig. 15 which are typical of what might be expected for a location south of the center of a westward electrojet. Adding this type of perturbation to the surge-related perturbation can easily produce the type of composite pattern shown in Fig. 13. Of course any electrojet has associated with it Birkeland current sheets and the connecting north-south current flow. There is now considerable evidence that there is a strong westward component of the electric field in the region behind the surge (Horwitz et al. 1978). This westward component of *E* drives both a westward Pedersen current and a northward Hall current. This northward Hall current would be expected to exceed by a considerable amount the southward Pedersen current which would be driven by the southward component of *E* normally found in the westward electrojet region. Thus one would expect to find the current flow to be northwestward in the region behind the surge.

All these above considerations were taken into account in designing a model current system to reproduce the magnetic field perturbation pattern associated with a surge. The model current system chosen is shown in Fig. 16. It consists of a westward electrojet with a longitudinal extent of *L* and a latitudinal width of *W*. This electrojet is considered to be a Hall current in the easternmost part of the system although the southwest orientation of the electric field sometimes makes it nearly a Cowling current. The westernmost part of the system is the site of intense downward fluxes of energetic electrons which represent a north-south aligned strip of negative charge. The electric field associated with this space charge distribution points eastward at the western edge of the surge and westward at the trailing edge of the surge. The upward current at the western edge of the electrojet is bled up over the surge region. Accordingly our model has a region of equatorward current flow of longitu-

dinal extent L_W at the western edge of the surge and a region of poleward current flow of longitudinal extent L_E at the trailing edge of the surge form (see Fig. 16). The north-south current is linked to the magnetosphere by Birkeland currents in the model. However it is quite possible that the northward and southward currents near the head of the surge are part of a Hall current vortex, as this would produce a magnetic perturbation pattern similar to the one produced by our three-dimensional system. Figure 17 shows sample latitude and longitude profiles computed for our model system along meridians and lines of constant latitude indicated in Fig. 16. The parameters for this model are given in Table 2. In this table, the west edge is defined as the longitude to the west of which no ionospheric current flows, that is the western edge of the region defined by L_W in Fig. 16. The total east-west length of the poleward/equatorward current system is given by $L_W + L_E$. Profile P covers the western edge of the surge and the region further west, Profile Q encompasses the entire surge form and Profile R emphasizes the eastern edge of the surge and regions further east of that. Each of these longitude profiles is taken at different latitudes to demonstrate how the position of the stations with respect to the electrojet can influence the observed perturbation pattern. The similarity of these profiles to the observational data we have presented in this paper is quite striking. The latitude profiles indicate how localized the positive D' regime can be, with that characteristic signature having disppeared completely in profile 3 at the trailing edge of the surge.

Finally we note that the calculations for the current systems were performed using the three-dimensional model systems de-

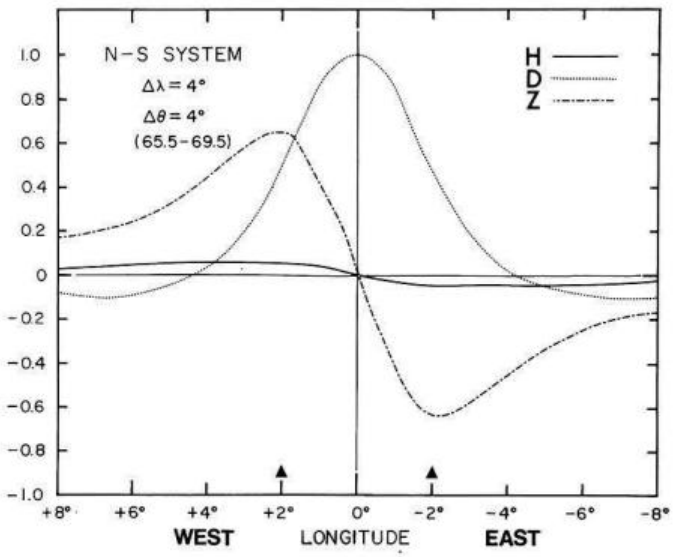

Fig. 14. Longitude profile showing the magnetic perturbation pattern for a three-dimensional current system involving a downward current sheet at 70.5° N, an upward current sheet at 66.5° N and equatorward flowing ionospheric current connecting the two field-aligned current sheets. The east-west extent of the current systems is 4°, the edges being indicated by triangles at ±2°. The profile is taken along 67.5° N

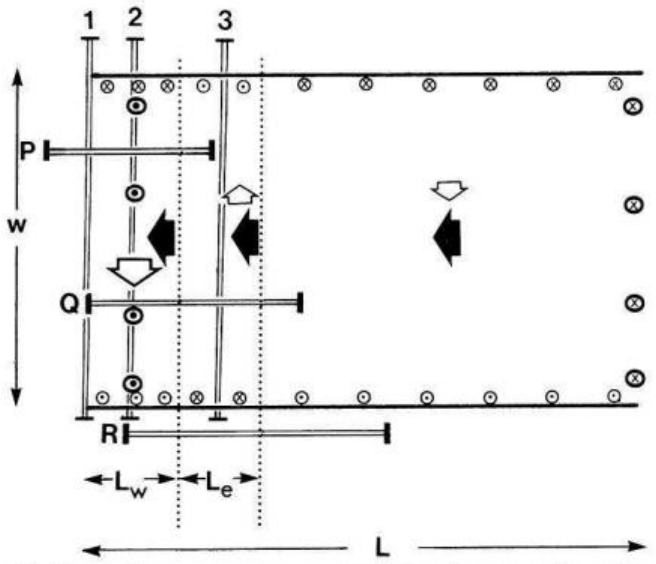

Fig. 16. Model current system proposed for the westward travelling surge and regions to the east of the surge. *P*, *Q*, and *R* refer to lines of constant latitude, along which theoretical longitude profiles are computed while 1, 2 and 3 refer to meridians along which theoretical latitude profiles are computed. The *solid arrows* indicate the direction of the east-west component of the ionospheric current, while the open arrows indicate the direction of the north-south current flow which connects the antiparallel Birkeland current sheets. Equatorward ionospheric current flows at the western edge of the surge region. The parameters shown in the figure are defined in the text. Parameters describing the actual system for cases computed in this study are shown in Tables 2 and 3

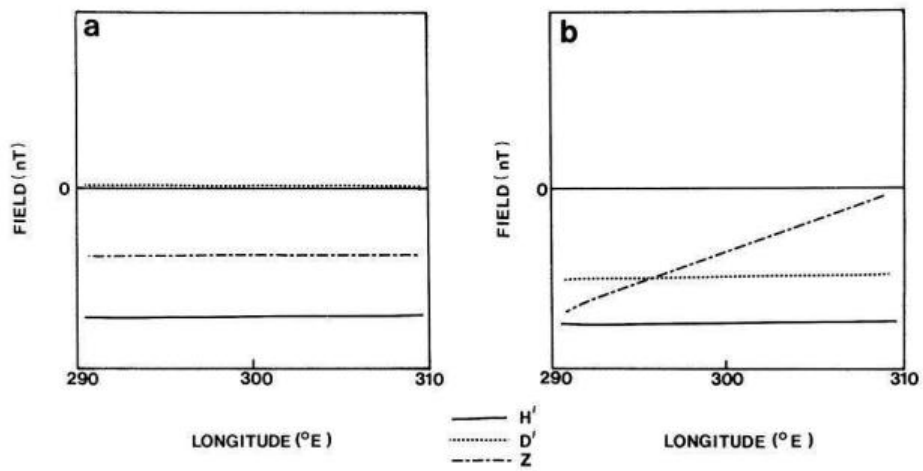

Fig. 15a, b. Schematic longitude profiles for an east-west array of field points to the south of a westward electrojet. For panel '**a**' the westward electrojet lies along lines of constant geomagnetic latitude while for panel '**b**' the electrojet runs from south-east to northwest at an angle to lines of constant geomagnetic latitude. Note that in the case depicted in panel '**b**' the negative D'-component can account, at least in part, for the negative D' behind the surge

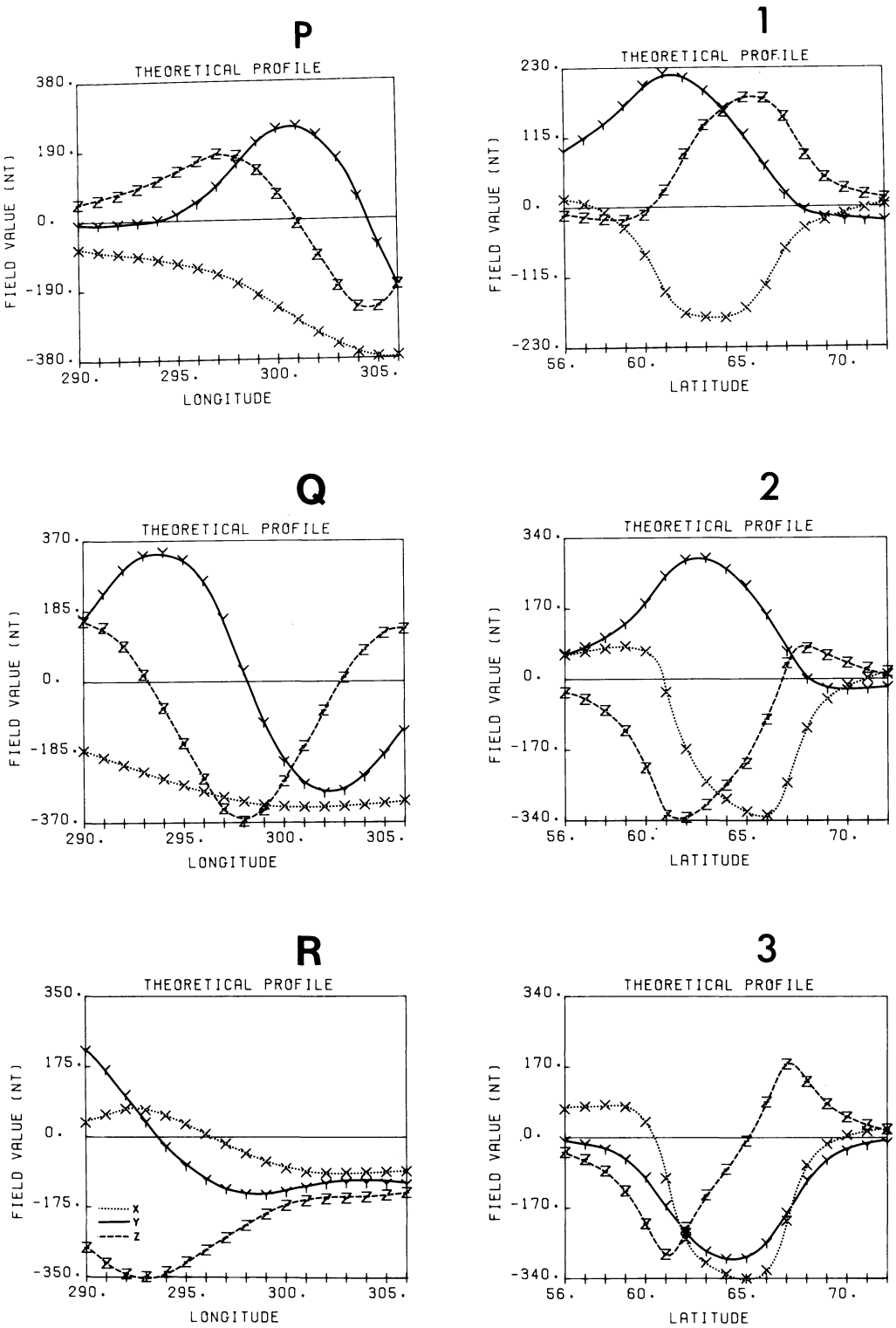

Fig. 17. Theoretical latitude and longitude sample profiles computed from the model current system shown in Fig. 16. Locations of the meridians *1*, *2* and *3* and lines of constant geomagnetic latitude *P*, *Q*, and *R* are shown in Fig. 16. Profiles *P*, *Q* and *R* are designed to show the effects of surge motion. At the same time the latitudinal variation of the perturbations is illustrated by allowing profiles *P*, *Q*, and *R* to be taken at different latitudes across the electrojet. The current system parameters are shown in Table 2

Table 2. Model current system parameters for production of profiles shown in Fig. 17

Poleward/equatorward current system			Westward current system		
West Edge Center (°E) (°N)	E-W Length (deg.)	N-S Width (deg.)	West Edge Center (°E) (°N)	E-W Length (deg.)	N-S Width (deg.)
290.0 65.0	10.0	6.0	290.0 65.0	20.0	6.0

veloped by Kisabeth and Rostoker (1977). For the model shown in Fig. 16 the ionospheric currents are at an altitude of 100 km and induction effects are simulated by placing a superconductor at depths below 200 km from the earth's surface. The ionospheric current density for each element of the system is 1 Am^{-1}.

(i) Model for Day 214, 1974

Figure 18 shows the observed longitude profiles chosen for model studies and the profiles obtained from the model whose parameters are shown in Table 3. One can see the increase in current density and the westward motion of the western edge of the

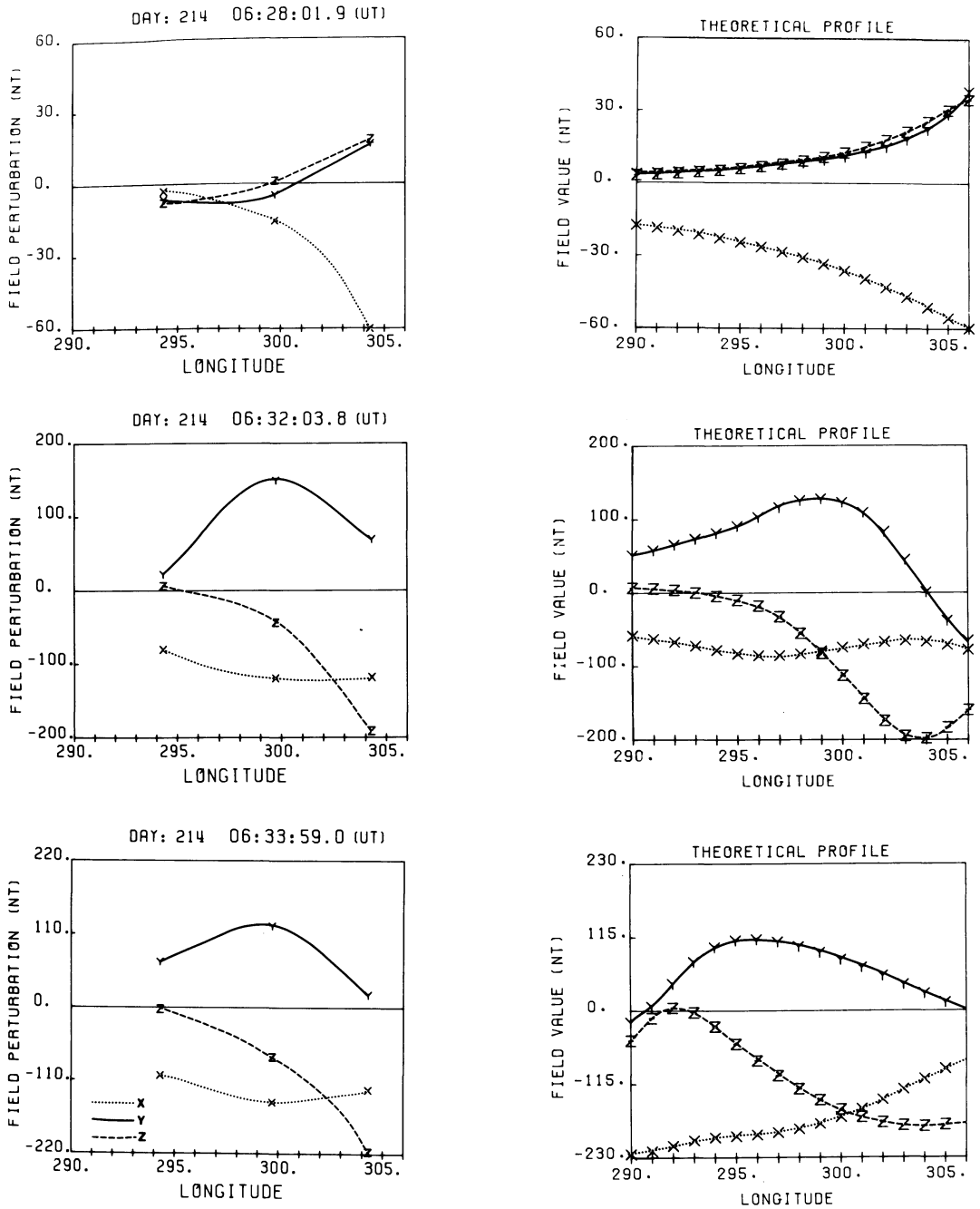

Fig. 18. Longitude profiles for observations made on Day 214, 1974 and the theoretical profiles which simulate them. *X*, *Y*, and *Z* indicate the geomagnetic north, east and vertical components. The current system parameters are shown in Table 3

Table 3. Model current system parameters for Day 214, 1974 and Day 307, 1976

	Poleward/Equatorward current system					Westward current system				
Profile	West Edge Center (° E) (° N)	E-W Length (deg.)	N-S Width (deg.)	Tilt (° east of south)	Current Density (Am^{-1})	West Edge Center (° E) (° N)	E-W Length (deg.)	N-S Width (deg.)	Tilt (° east of south)	Current Density (Am^{-1})
Day 214/74										
B	308.0 68.0	14.0	6.0	0	0.25	308.0 68.0	20.0	6.0	0	0.35
D	296.5 70.0	14.0	6.0	0	0.40	294.0 70.0	25.0	6.0	0	0.45
E	278.0 69.5	12.0	7.0	−10	0.90	278.0 69.5	30.0	7.0	−10	0.70
Day 307/76										
A						290.0 67.5	25.0	4.0	20	0.20
B1	292.0 71.5	19.0	6.0	20	0.55	290.0 71.5	25.0	6.0	20	0.12
D6	284.0 72.5	20.0	7.0	20	0.45	284.0 72.5	26.0	7.0	20	0.50
E						278.0 72.5	30.0	7.0	20	0.75

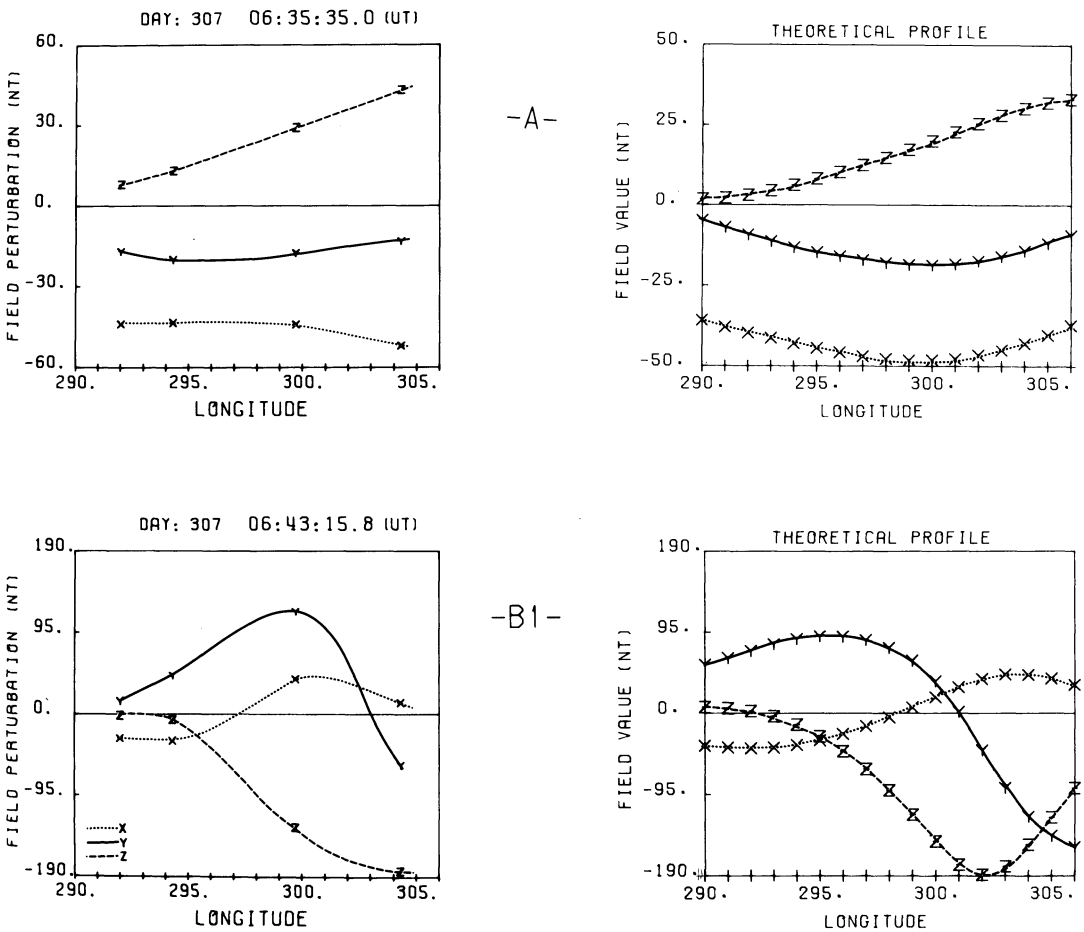

Fig. 19. Longitude profiles for observations made early in the event recorded on Day 307, 1976 and the theoretical profiles which simulate them. Note that profile *A* is taken before the arrival of the surge while profile E is taken after the surge form has disappeared from the Alberta sector. In both cases, only the westward current system is needed to model the magnetic effects. The current system parameters are shown in Table 3

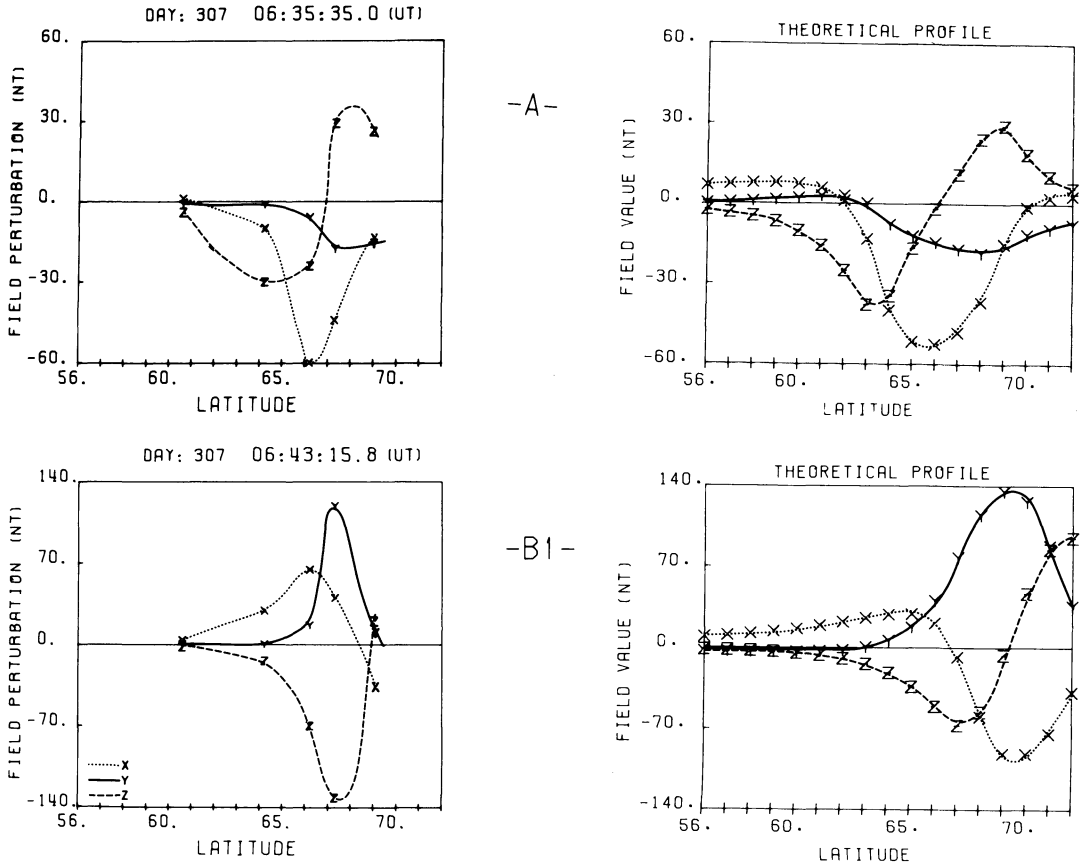

Fig. 20. Latidude profiles for the same instants during the event on Day 307, 1976 presented in Fig. 19

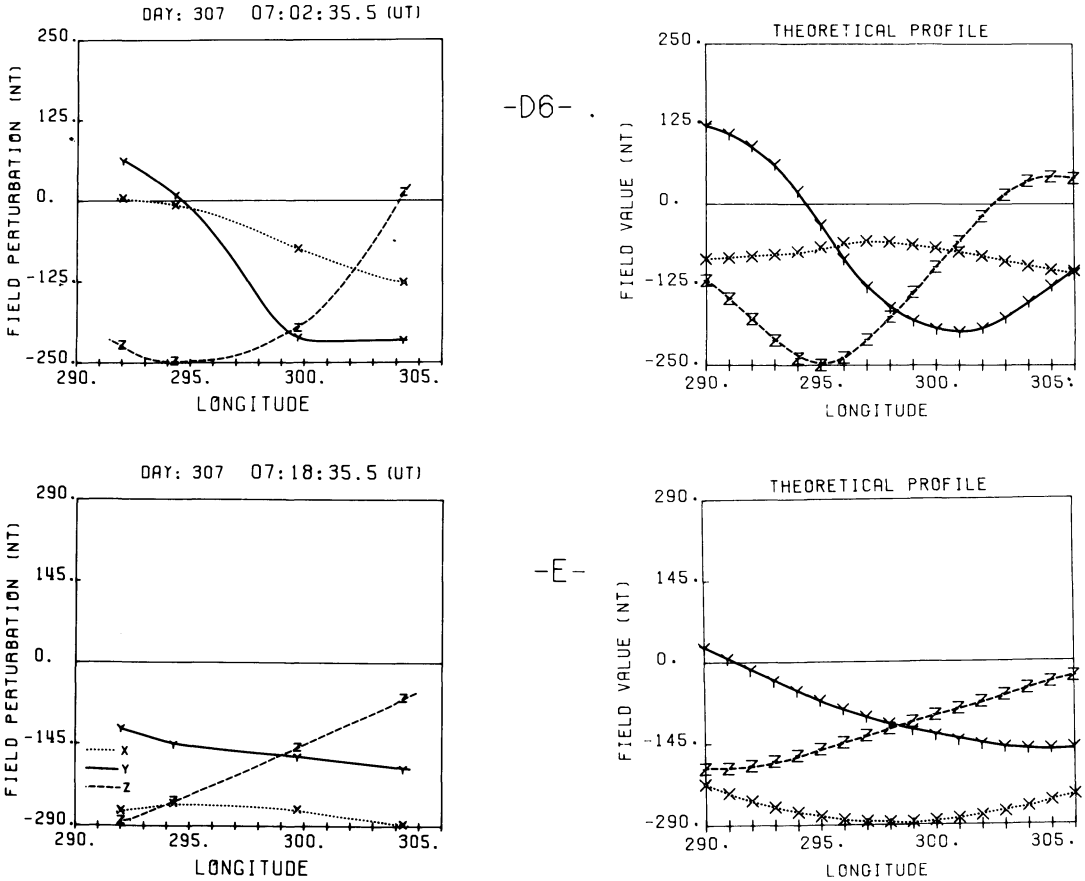

Fig. 21. Longitude profiles for observations later in the event recorded on Day 307, 1976 and the theoretical profiles which simulate them. The current system parameters are shown in Table 3

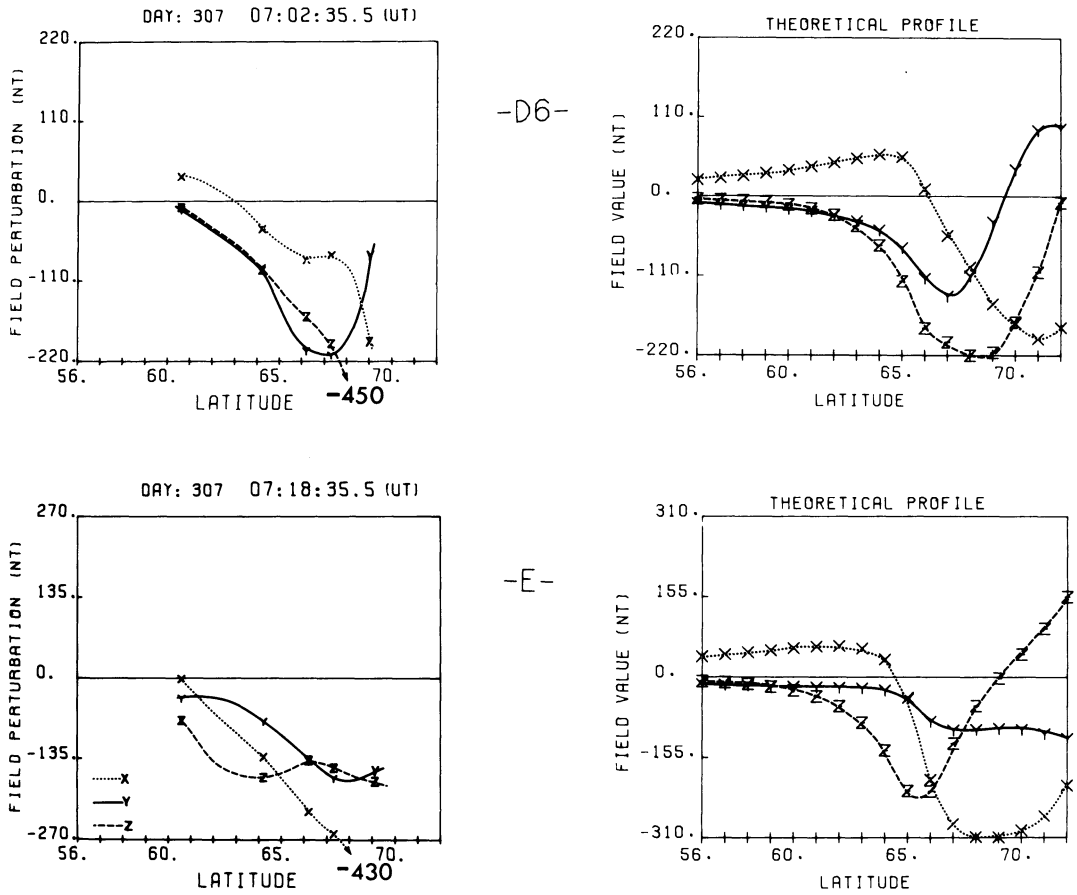

Fig. 22. Latitude profiles for the same instants during the event on Day 307, 1976 presented in Fig. 21. The maximum negative H'-component at YKNF is off-scale. Good agreement of the model at YKNF is not expected since YKNF is several degrees to the west of the Alberta meridian line and marked azimuthal asymmetries occur in the vicinity of the surge

surge as the event develops. Clearly the head of the surge is to the east of Uranium City at the onset of the event but has moved west of Fort Providence by 0633:39. There are obviously some discrepancies between the model results and the observations, but this is to be expected in the light of the fact that we cannot faithfully reproduce the true current distribution in so complex a situation as a substorm disturbance.

(ii) Model for Day 307, 1976

For this case we shall use our model to produce latitude and longitude profiles, as both types of observational data were available for this event which was recorded while the Alberta IMS array was in operation. Figures 19 and 20 show sample longitude and latitude profiles. The model parameters are shown in Table 3. It will be noted that the profile at 0635:35 was taken prior to the arrival of the surge while that at 0643:15 was taken after the surge had developed in the Alberta sector. We consider the overall agreement between the model and observations to be particularly good in these cases, given the complexity of substorm disturbances.

The profiles in Fig. 21 and 22 represent the situation after the passage of the surge. The model parameters are again given in Table 3. While agreement for the longitude profiles (Fig. 21) seems reasonable, there are clear discrepancies in the case of the latidue profiles which might be expected considering the fact that all the stations are not truly on the same meridian (e.g., the longitude of Fort McMurray is 303.3° E while the longitude of Yellowknife is 292.6° E). In addition, given the sharp spatial changes in the substorm perturbation pattern particularly in the vicinity of the surge, outstanding agreement should not be expected. In fact, this is a good indicator of how careful one must be in ensuring that stations used for meridian line profiles do not deviate significantly from a common meridian.

Discussion and Conclusions

The purpose of this research was to investigate the current configuration associated with the westward travelling surge and to trace the development of the surge form through following the spatial and temporal development of its current system. This paper is the first to utilize constraints provided by knowledge of the variation of the magnetic perturbation pattern as a function of longitude, and the longitude profiles presented are the first such profiles published in the literature to date. Using this information we can study the longitudinal motion of surge forms and gain some measure of knowledge of the longitudinal scale size of the current carrying regions. Based on the analysis presented in this paper we have reached the following conclusions.

(i) The motion of Surges

There seem to be many different ways in which a surge can develop and behave. Traditionally one considers the surge as

representing the head of a westward electrojet as it expands westward during the substorm expansion phase. Certainly, as in the case of Day 214, 1974, we have encountered cases where the surge had developed to the east of the Alberta sector and had moved westward across our sector at the head of an expanding westward electrojet. On a time scale of minutes this motion may be very irregular, and at times the surge may stop propagating for a few minutes before resuming its motion.

On the other hand, we have observed surge forms develop in which the current magnitude grows and decays without any significant westward expansion being observed (as observed early in the event on Day 307, 1976). In the cases we have studied, such surge forms tend to appear before the arrival of the substorm intensified-westward electrojet in our sector.

One may attempt to understand this surge behaviour in the following fashion. The westward electrojet connects regions of net downward field-aligned current flow in the noon sector to regions of net upward field-aligned current flow in the pre-midnight sector. The concept of the downward field-aligned current of the portion of the substorm three-dimensional current loop is implicit in the model studies of Rostoker and Hughes (1979). It is adopted because there appears to be no indication of strong net downward field-aligned current in the region just to the east of the average substorm disturbed region which would be identified by a positive level shift in the east-west component of the perturbation magnetic field going from south to north across the oval. It is, of course, possible that there is a net downward current to the east of the surge, however it would be distributed over a large longitude range resulting in a weak effect in the region of the surge. Since we are trying to model only the perturbation field in the near vicinity of the surge, we do not include any net downward current east of the surge in the model. The surge, itself, represents a region of intense upward field-aligned currents which are carried by keV electrons in the region below the acceleration region (Mozer et al. 1980). While the upward flow of cold ionospheric electrons in the noon sector can easily account for the net downward field-aligned current observed in that region, it is more difficult to explain the flow of upward current in the pre-midnight sector. It is presently felt that upward current is carried by the hot electrons which have been accelerated above the ionosphere by parallel electric fields, and that the acceleration is needed to give the electrons a sufficiently high velocity so as to provide the maximum possible current densities. The equation of continuity provides a limitation as to how large this current density can be and thus, in order to match the nightside upward field-aligned current to the dayside downward field-aligned current, it is necessary for the region of upward field-aligned current to expand in ionospheric cross sectional area. The growth of a surge region represents the development of a new section of the ionosphere from which upward field-aligned current may flow. For reasons which are presently not well understood, it would appear that regions of upward current flow (marked by discrete auroral arcs) attain limited latitudinal scale size. Development of discrete auroras involves the sudden creation of new auroral arcs rather than the continual growth in size of a single arc. The suddenness of discrete arc development is symptomatic of the substorm process and differs form the smooth appearance of increases in downward field-aligned current across the noon sector. Insofar as the actual development of a surge is concerned, initially the growth of the current density may satisfy the need for the magnetosphere to balance the upward and downward flow, so that the strength of the current in the surge may grow with no further growth of the area occupied by the surge. In that case, the surge will simply intensify while showing no westward expansion. In other cases, the increase in downward current on the dayside may be so large that the development of a new surge region may be inadequate in terms of the ionospheric cross sectional area available and it will be necessary for the surge to expand westward. In essence, therefore, the motion of the surge region reflects the changes in downward current flow on the dayside in order to maintain current continuity in the magnetosphere/ionosphere current circuit. The most rapid spatial development of the surge would be expected to be associated with the strongest enhancements in current flow in the auroral oval.

(ii) The Scale Size of Surges

The analysis of the longitude profiles in the vicinity of westward travelling surges has allowed us, using modelling techniques, to estimate the east-west scale size of the surge region for several events. The data for these estimates are found in Table 3 where the length of the poleward/equatorward current system at the head of the westward electrojet represents the east-west extent of the surge region. Table 3 shows the estimates for five separate surge events of varying current strengths. It is seen that the east-west extent ranges between 12°–20° at a latitude of approximately 70° N which amounts to a range of 455–760 km. According to our model, equatorward ionospheric current will flow in the western half of this region with poleward current flowing in the eastern half. Thus the east-west scale size of the region of equatorward current flow at the head of the surge would appear to be of the order of 230–380 km. Since the ground magnetometers are a minimum of 100 km away from the current-carrying region at all times, a region of width 230 km can be considered to be rather narrow in terms of the resolving power of ground based magnetometer arrays. For one to detect the surge region, it is necessary to have a magnetometer at the correct latitude and within approximately 500 km of the surge in an east-west direction before one can be sure of detecting the traditional positive D'-component perturbation associated with the surge.

Knowledge of the east-west scale size of surge regions allows us to make some estimate of the scale size of the substorm disturbed region in the magnetotail, which in turn reflects the probability of a satellite in the tail region finding itself in the volume of space to which the surge region maps. Rostoker and Boström (1976) developed mapping factors from the ionosphere to the magnetotail based on the contention that the Birkeland current region as observed just above the ionosphere mapped the half-width of the plasma sheet in the tail. Based on their contention, the mapping factor for the azimuthal direction was 56. Using this factor and the model calculations shown in Table 3, the azimuthal extent of the surge region in the magnetotail should be of the order of 34,000 km or 5.3 R_E. Since the tail has an average width of about 40 R_E, it can be seen that the surge region involves only about 10%–15% of the tail insofar as its azimuthal extent is concerned.

There is no doubt that the model for the surge presented in this paper is relatively crude. No effort was made to greatly refine the model so as to produce an optimum model based on some quantitative criterion involving the deviation of each model prediction from the observation. The relatively small number of stations used in data acquisition make such an effort unprofitable. Only the exploitation of two-dimensional array data such as that which has been recently acquired in the European sector over the period of the International Magnetospheric Study will make such improvements in analysis worthwhile to

undertake. In fact, a recent study by Inhester et al. (1981) has utilized two-dimensional magnetometer array data and auroral zone electric field data acquired by STARE to develop a model for the surge which is in good agreement with the results presented in our present study.

Acknowledgements. We would like to thank Drs. K. Kawasaki, J.V. Olson, and T.J. Hughes for useful discussions during the course of this research. We are greatly indebted to Transport Canada (Telecommunications Branch), to the Atmospheric Environment Service (Western Regional Headquarters) and to Mr. and Mrs. Ted Malewski of Fort Providence, Northwest Territories, for their help in arranging for the operation of the University of Alberta array. Standard magnetogram data were provided by World Data Center-A for the Solar Terrestrial Physics and by Earth Physics Branch of Dept. of Energy Mines and Resources of Canada. This research was supported by the Natural Sciences and Engineering Research Council of Canada.

References

Akasofu, S.-I.: The development of the auroral substorm. Planet. Space Sci. **12**, 273–282, 1964

Akasofu, S.-I., Meng, S.-I., Kimball, D.S.: Dynamics of the aurora – IV polar magnetic substorms and westward traveling surges. J. Atmos. Terr. Phys. **28**, 489–496, 1966

Baumjohann, W.: Spatially inhomogeneous current configurations as seen by the Scandinavian magnetometer array. In: Proceedings of the International Workshop on Selected Topics of Magnetospheric Physics, Tokyo. March, 1979

Chen. A.J., Rostoker, G.: Auroral polar currents during periods of moderate magnetospheric activity. Planet. Space Sci. **22**, 1101–1115, 1974

Horwitz, J.L., Doupnik, J.R., Banks, P.H.: Chatanika radar observations of the latitudinal distributions of auroral zone electric fields, conductivities and currents. J. Geophys. Res. **83**, 1463–1481, 1978

Inhester, B., Baumjohann, W., Greenwald, R.A., Nielsen, E.: Joint two-dimenstional observations of ground magnetic and ionospheric electric fields associated with auroral zone currents. 3. Auroral zone currents during the passage of a westward travelling surge. J. Geophys. **49**, 155–162, 1981

Kawasaki, K., Rostoker, G.: Perturbation magnetic fields and current systems associated whith eastward drifting auroral structures. J. Geophys. Res. **84**, 1464–1480, 1979a

Kawasaki, K., Rostoker, G.: Auroral motions and magnetic variations associated with the onset of auroral substorms. J. Geophys. Res. **84**, 7113–7122, 1979b

Kisabetz, J.L.: The dynamical development of the polar electrojets. Ph. D. Thesis, University of Alberta, Edmonton, Alberta, Canada, 1972

Kisabeth, J.L., Rostoker, G.: Current flow in the auroral loops and surges inferred from ground-based magnetic observations. J. Geophys. Res. **79**, 5573–5584, 1973

Kisabeth, J.L., Rostoker, G.: Modelling of three-dimensional current systems associated with magnetospheric substorms. Geophys. J.R. Astron. Soc. **49**, 655–683, 1977

Meng, C.-I.: Polar magnetic and auroral substorms. M. Sc. Thesis, University of Alaska, 1965

Mozer, F.S., Cattell, C.A., Hudson, M.K., Lysak, R.L., Temerin, M., Torbert, R.B.: Satellite measurements and theories of low altitude auroral particle acceleration. Space Sci. Rev. **27**, 155–213, 1980

Pytte, T., McPherron, R.L., Kokubun, S.: The ground signatures of the expansion phase during multiple onset substorms. Planet. Space Sci. **24**, 1115–1132, 1976

Rostoker, G., Boström, R.: A mechanism for driving the gross Birkeland current configuration in the auroral oval. J. Geophys. Res. **81**, 235–244, 1976

Rostoker, G., Hughes, T.J.: A comprehensive model current system for high latitude magnetic activity. 2. The substorm component. Geophys. J. **58**, 571–581, 1979

Rostoker, G., Akasofu, S.-I., Foster, J., Greenwald, R.A., Kamide, Y., Kawasaki, K., Lui, A.T.Y., McPherron, R.L., Russell, C.T.: Magnetospheric substorms – definition and signatures. J. Geophys. Res. **85**, 1663–1668, 1980

Tighe, W.G.: The development of the westward travelling surge during magnetospheric substorms. M.Sc. Thesis, University of Alberta, Fall, 1979

Wiens, R.G., Rostoker, G.: Characteristics of the development of the westward electrojet during the expansive phase of magnetospheric substorms. J. Geophys. Res. **80**, 2109–2128, 1975

Received November 3, 1980; Revised version June 22, 1981
Accepted June 23, 1981